Supporting information

Delivering Mechanism of Doxorubicin by the PEG-DPPE Micelles on Membrane Invasion by Dynamic Simulations

Lina Zhao, Meina Ren, Yanjiao Wang, Hailong An*, Fude Sun*

Key Laboratory of Molecular Biophysics, Hebei Province, Institute of Biophysics, School of Health Science & Biomedical Engineering, Hebei University of Technology, Tianjin, 300401, China

Respondence: sunfd@hebut.edu.cn; hailong_an@hebut.edu.cn.

Model Setup

CG model building of doxorubicin molecule

The system was energy minimized for 3000 steps by *steepest* method. It was then pre-equilibrated by temperature coupling with *v-rescale* method as the reference temperature of 300 K and a time constant of 0.1 ps. The pressure coupling was conducted with *parrinello-rahman* method and the reference pressure of 1.0 bar, a compressibility of 4.6×10^{-5} bar^{-1} and a time constant of 0.5 ps. The coupling type was set as *isotropic* in all the three dimensions. The non-bonded coulomb and the Vdw interactions were both switched from 0 to 1.4 nm where the force deceased to zero. The timestep was set as 1 fs and the MD ran for a duration of 10 ns. The CG structural parameters were fitted based on the AA data, and trials of CG simulations of solvated DOX in an $8\times8\times8$ nm^3 box were carried on to optimize the structural parameters, allowing for a stable simulation of CG DOX in a 20 fs timestep. The CG system was energy minimized and equilibrated by the same coupling methods as above. Note that the pressure coupling details changed to a compressibility of 3×10^{-6} bar^{-1} and a time constant of 8 ps. The Coulomb and Vdw interactions adopted a shift cut-off method that the former decreased to zero from 0 to 1.2 nm while the latter decreased to zero from 0.9 to 1.2 nm. A timestep of 20 fs was applied and the simulation continued for 200 ns. For validation, 15 DOXs in AA and CG conditions were respectively filled in a box with size of $8\times8\times8$ nm^3 and productions were carried on for 200 ns. The simulation details kept the same with description above. And the gro and itp of CG DOX were put in supporting information (TableS1, TableS2).

Free energy calculation of drug in membrane permeation

The free energy of permeation of doxorubicin in different systems across model apical lipid layer were calculated by umbrella sampling method. During the pulling process, the phospholipid tails of membrane molecules were restricted in position by a harmonic potential of 1000 kJ · mol^{-1} · nm^{-2} in all three dimensions. Different systems were created with different numbers of separated windows within a pulling distance to generate well-overlapping configuration distributions (Fig. S13). Each window was then equilibrated for 200 ns with the force constant of 1500 kJ · mol^{-1} · nm^{-2}, followed by a 2.0 μs production simulation. The association energy was computed with the Weighted Histogram Analysis Method (*J. Comput. Chem., 2012, 33, 453-465*). Statistical errors were estimated with bootstrap analysis. The complete histograms were considered as the independent data points to which random weights were assigned for bootstrap.

Calculation method

The contact intensity was calculated by tool of *gmx mindist* where any molecules in the analyzing group within the cutoff distance of 0.6 nm from the reference group were counted as contact intensity. The cutoff distance was consistent with lipid contacting analysis in a previous study (*Biophys. J. 2018, 114, 1858–1868*).

Order parameter of lipids are used to calculate and observe the structural orientation of monolayer membranes. The reduction of the order parameter implies a transition of the lipid from the ordered phase to the disordered phase. The average lipid ordering parameter varied between -0.5 and 1. Value of 1 indicates perfect alignment of lipids with the bilayer normal. -0.5 indicates anti-alignment. And the order parameter of the lipid molecules is calculated using the following equation:

$$Sz = \frac{1}{2}\left(3 < \cos\theta^2 > - 1\right)$$

Where *Sz* stands for order parameter, "θ" is the angle between the bond and the bilayer normal, and the angle bracket indicates the average value over time.

1V3OU	B1	1	3.211	2.801	3.649	0.3861	0.3868	-0.0945
1V3OU	B2	2	3.482	2.744	3.621	0.7285	0.0956	-0.2867
1V3OU	B3	3	3.167	3.073	3.579	-0.3978	0.0406	-0.1006
1V3OU	B3	4	3.500	3.032	3.480	-0.2313	0.1933	0.3895
1V3OU	B4	5	3.109	3.151	3.340	-0.3110	0.0050	-0.1333
1V3OU	B4	6	3.429	3.123	3.250	-0.1909	-0.0145	0.2938

1V3OU	B5	7	3.229	3.180	3.140	-0.1223	-0.5187	-0.0992
1V3OU	B5	8	3.219	3.165	2.925	-0.0641	0.0369	-0.1438
1V3OU	B6	9	2.956	3.294	3.011	0.3958	0.1578	-0.0167
1V3OU	B1	10	3.038	2.632	3.777	-0.0547	0.0847	0.0204
1V3OU	B7	11	2.862	2.455	4.019	0.0204	-0.1856	-0.1225
1V3OU	B8	12	3.234	2.481	3.931	0.0137	0.0747	-0.0764
1V3OU	B9	13	3.688	2.592	3.705	0.2409	-0.1331	0.1010

Table S1. Information of the .gro file of CG DOX.

[moleculetype]							
Name	nrexcl						
Doxorubicin	1						
[atoms]							
nr	type	resnr	resid	atom	cgnr	charge	mass
1	SC5	1	DOX	B1	1	0.000	45.000
2	SP1	1	DOX	B2	2	0.000	45.000
3	SP2	1	DOX	B3	3	0.000	45.000
4	SP2	1	DOX	B3	4	0.000	45.000
5	SNa	1	DOX	B4	5	0.000	45.000
6	SNa	1	DOX	B4	6	0.000	45.000
7	SC4	1	DOX	B5	7	0.000	45.000
8	SC5	1	DOX	B5	8	0.000	45.000
9	N0	1	DOX	B6	9	0.000	72.000
10	SC5	1	DOX	B1	10	0.000	45.000
11	Nda	1	DOX	B7	11	0.000	45.000
12	Qd	1	DOX	B8	12	1.000	72.000
13	P3	1	DOX	B9	13	0.000	72.000
[constraints]							
i j	funct	bond					
3 4	1	0.350					
5 6	1	0.334					
4 6	1	0.258					
3 5	1	0.258					
5 7	1	0.235					
6 7	1	0.235					
7 8	1	0.216					
10 11	1	0.347					
10 12	1	0.292					
11 12	1	0.353					
[bonds]							
i j	funct	dis	fc				
1 2	1	0.262	20000				
1 3	1	0.278	20000				
2 4	1	0.315	20000				

7 9	1	0.285	20000	
8 9	1	0.336	20000	
1 10	1	0.285	20000	
2 13	1	0.287	20000	
[angles]				
i j	ak	funct	angle	fc
1 2	4	1	90.16	50.00
3 1	2	1	106.3	50.00
7 8	9	1	57.50	50.00
7 9	8	1	39.60	50.00
4 2	13	1	129.3	50.00
2 1	10	1	123.3	50.00
10 11	12	1	65.66	50.00
10 12	11	1	55.37	50.00
1 10	12	1	92.86	50.00
6 7	8	1	102.6	50.00
[dihedrals]				
i j k l	funct	angle	fc	
1 2 4 3	2	0.00	100	
1 2 6 5	2	0.00	100	
5 6 8 9	2	0.00	100	
4 3 9 7	2	0.00	100	
1 2 4 5	2	0.00	100	
#ifdef POSRES #ifndef POSRES_FC #define POSRES_FC 1000.00 #endif [position_restraints]				
1	1	POSRES_FC	POSRES_FC	POSRES_FC
2	1	POSRES_FC	POSRES_FC	POSRES_FC
3	1	POSRES_FC	POSRES_FC	POSRES_FC
4	1	POSRES_FC	POSRES_FC	POSRES_FC
5	1	POSRES_FC	POSRES_FC	POSRES_FC
6	1	POSRES_FC	POSRES_FC	POSRES_FC
7	1	POSRES_FC	POSRES_FC	POSRES_FC
8	1	POSRES_FC	POSRES_FC	POSRES_FC
9	1	POSRES_FC	POSRES_FC	POSRES_FC
10	1	POSRES_FC	POSRES_FC	POSRES_FC
11	1	POSRES_FC	POSRES_FC	POSRES_FC
12	1	POSRES_FC	POSRES_FC	POSRES_FC
13	1	POSRES_FC	POSRES_FC	POSRES_FC
#endif				

Table S2. Information of the .itp file of CG DOX.

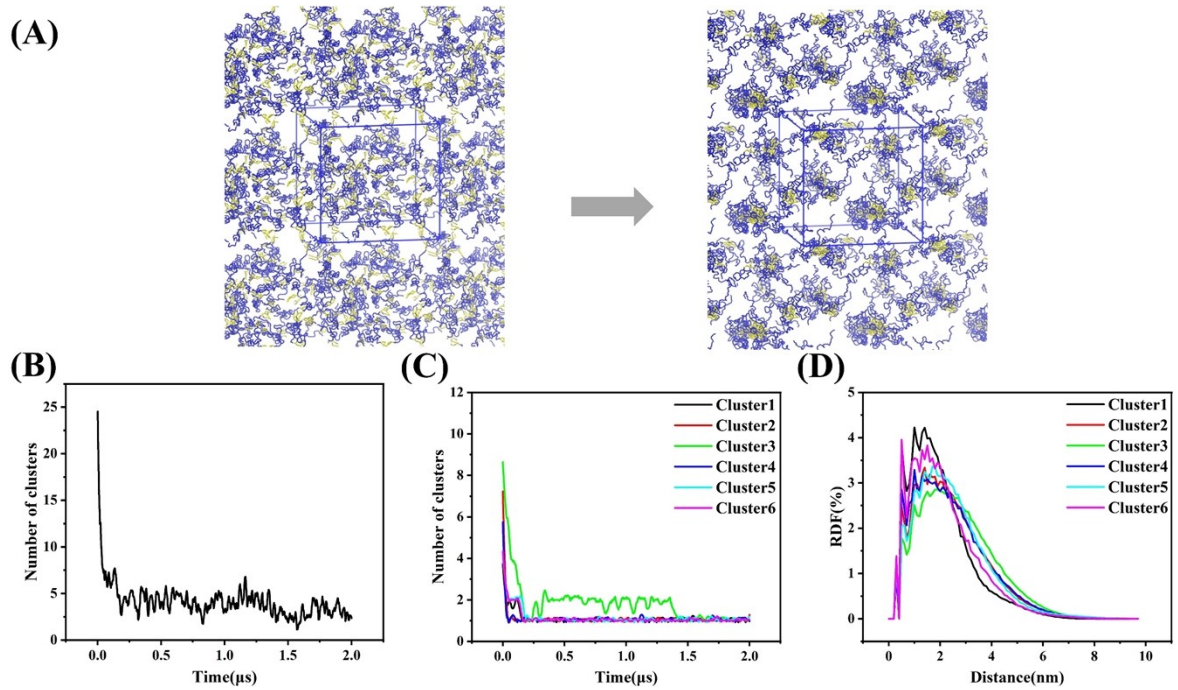

Figure S1. (A) Initial and final states of PEG2000-DPPE micelle assembly. The PEG2000-DPPE micelle was generated from a simulation production of 80 PEG2000-DPPE monomer molecules solvated by water, which was proved to assemble into the micelle-like clusters. (B) Change in the number of aggregates in the box. (C) Change in the number of clusters of different aggregates over a time of 2 μs. (D) Radial distribution function of the hydrophilic shell around the hydrophobic core of each aggregate.

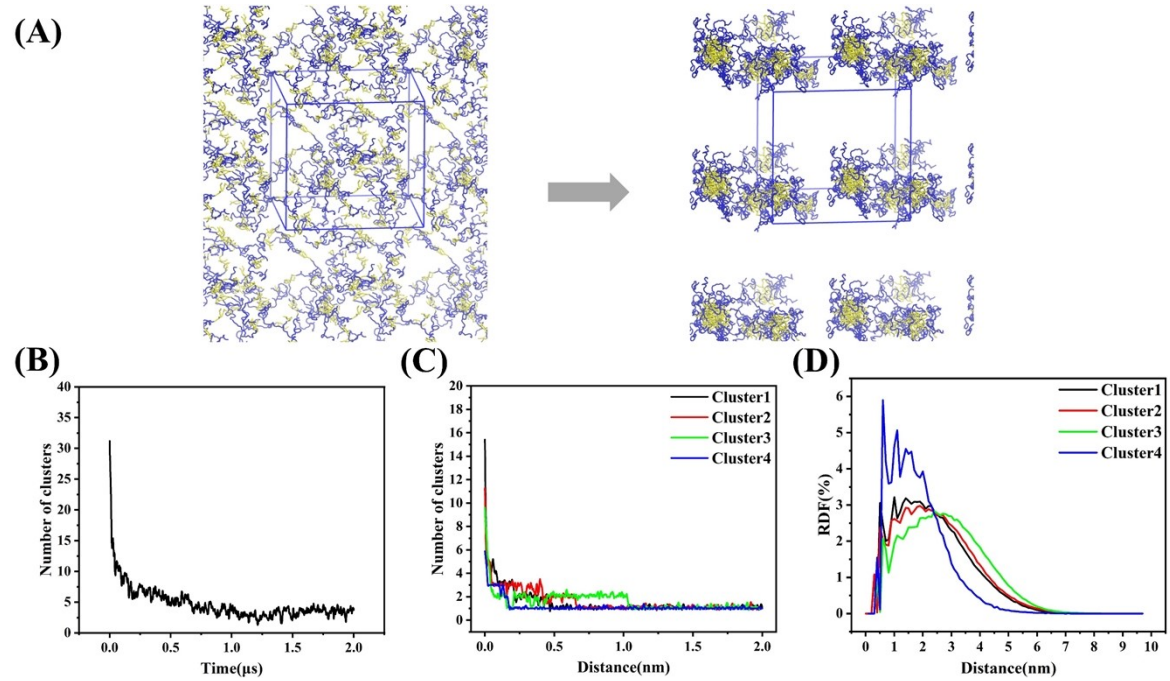

Figure S2. (A) Initial and final states of PEG1250-DPPE micelle assembly. The PEG1250-DPPE micelle was also generated from a simulation production from a state that 80 PEG1250-DPPE

monomer molecules solvated by water randomly distributed in a cubic box. (B) Change in the number of aggregates in the box. (C) Change in the number of clusters of different aggregates over a time of 2 μs. (D) Radial distribution function of the hydrophilic shell around the hydrophobic core of each aggregate.

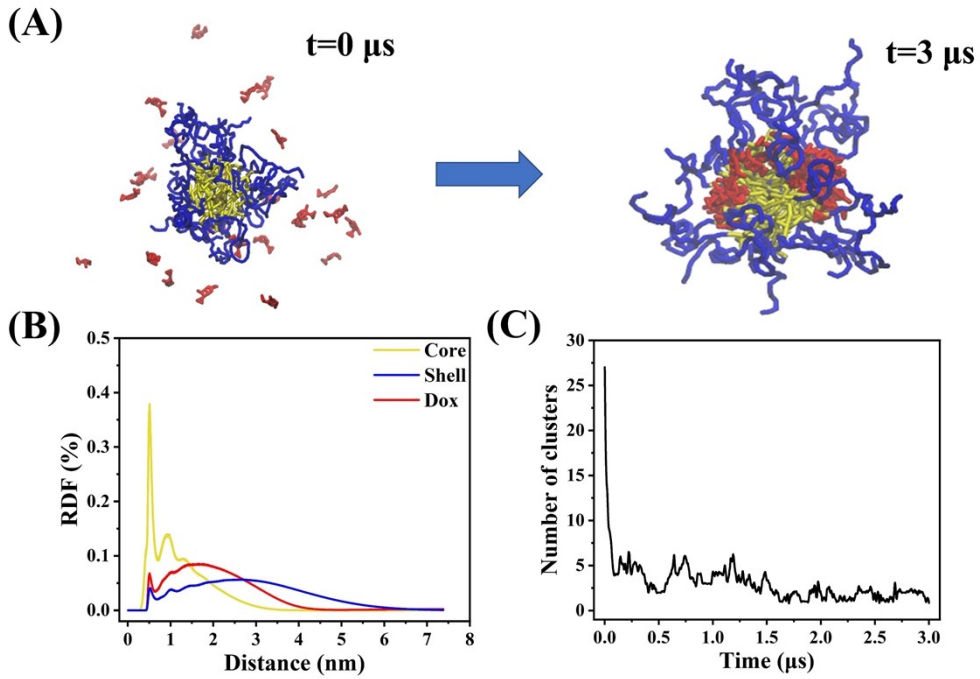

Figure S3. DOX-loaded PEG1250-DPPE micelle and characterization of the drug distribution. (A) Snapshots of the doxorubicin position relative to the PEG1250-DPPE micelle system in the initial and final states are shown. The hydrophilic PEG and the hydrophobic DPPE were shown in blue and yellow respectively. (B) RDFs of the DPPE moieties, PEG bunches and doxorubicin relative to the lipid tail of the micelle. (C) Evolution of the cluster number of doxorubicin molecules during interacting with the micelle.

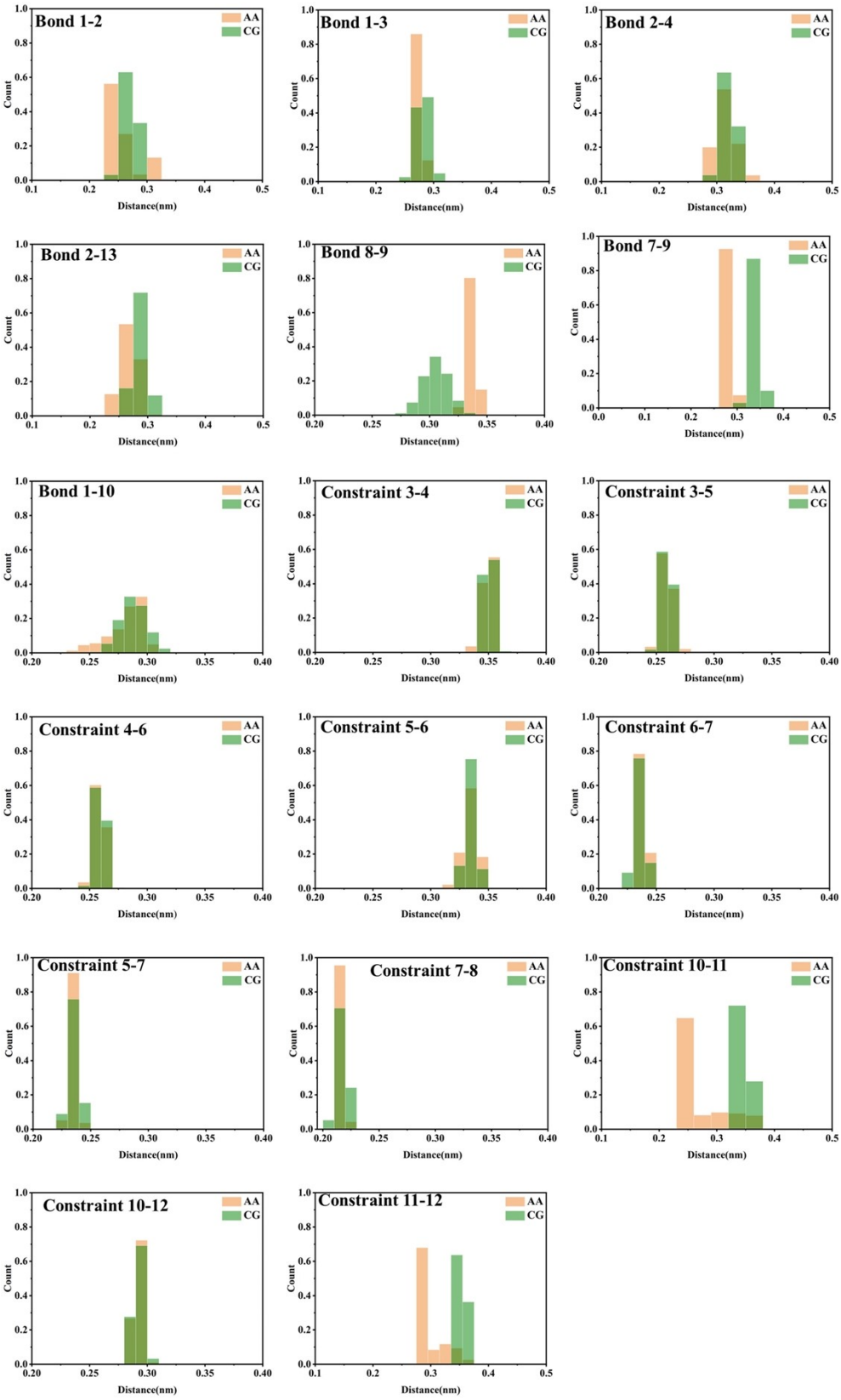
Bond 1-2
Bond 1-3
Bond 2-4
Bond 2-13
Bond 8-9
Bond 7-9
Bond 1-10
Constraint 3-4
Constraint 3-5
Constraint 4-6
Constraint 5-6
Constraint 6-7
Constraint 5-7
Constraint 7-8
Constraint 10-11
Constraint 10-12
Constraint 11-12
AA
CG
Count
Distance(nm)

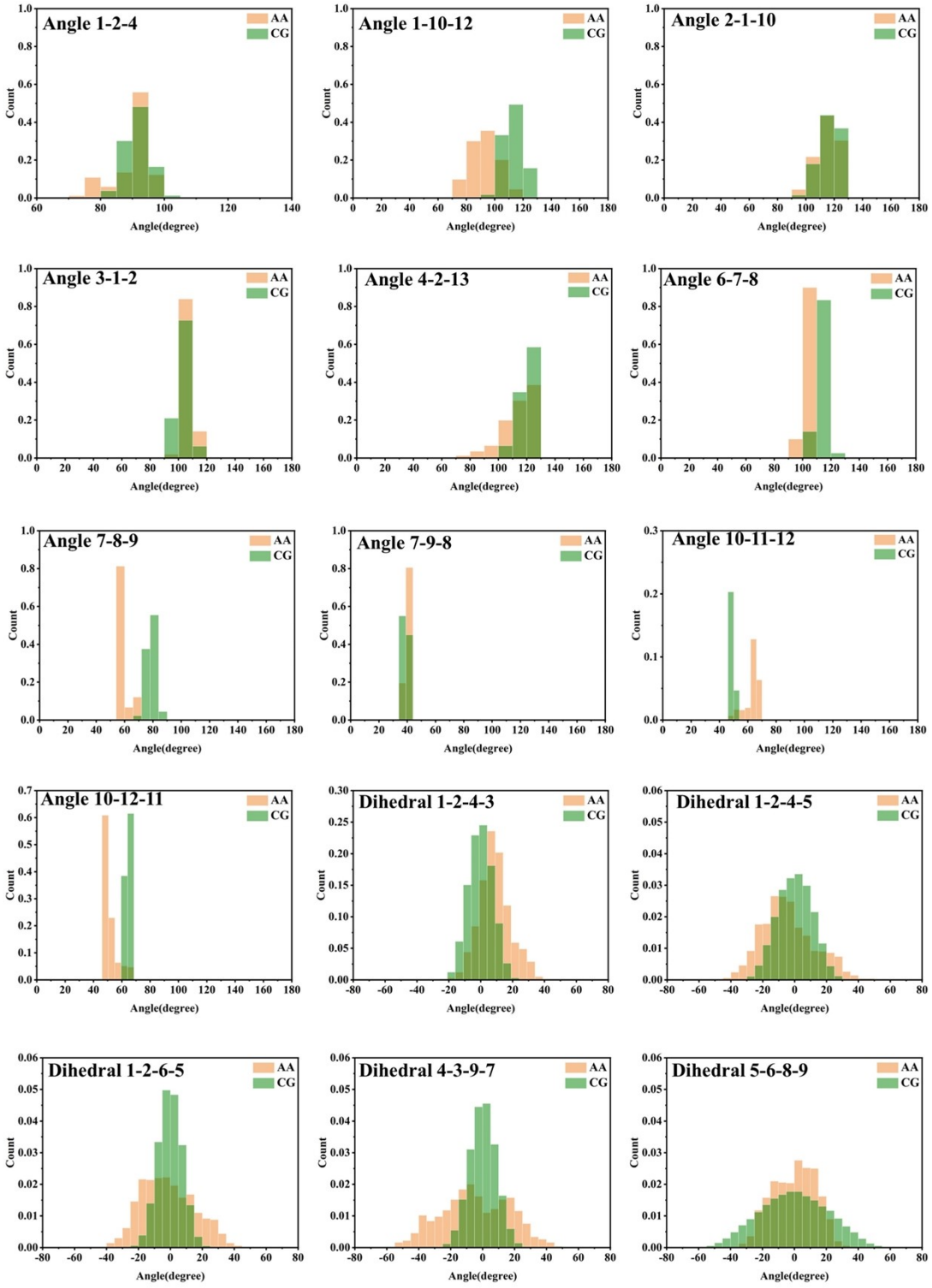

Figure S4. Comparison of bond lengths, angles and dihedral of DOX molecule between the AA and CG models.

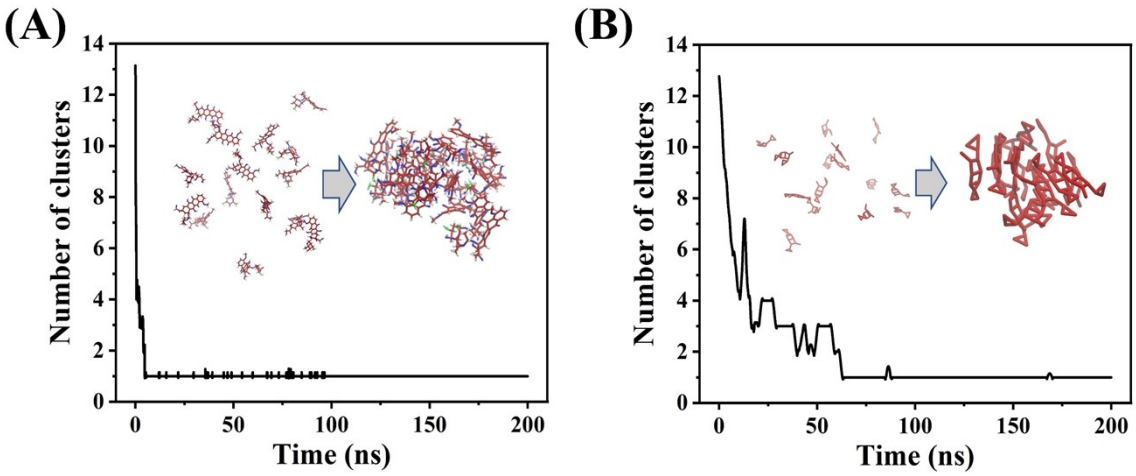

Figure S5. A comparison of DOX clustering evolutions of AA (A) and CG (B) models, respectively. Any two DOX molecules were classified into one cluster if the distance of them was less than 0.55 nm.

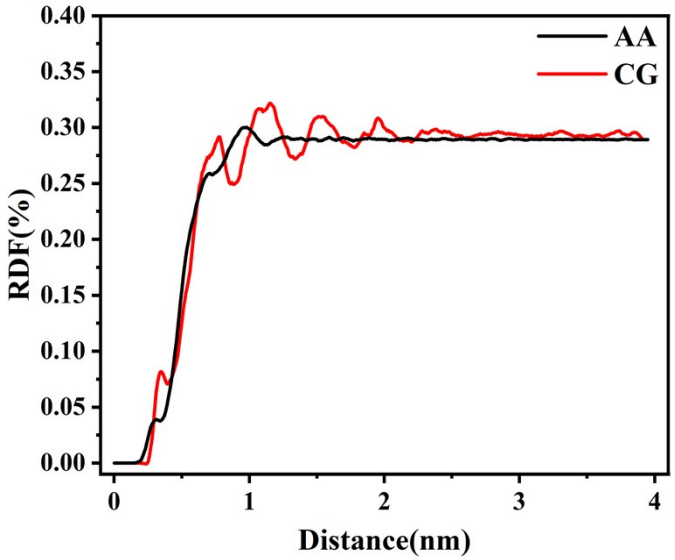

Figure S6. The radial distribution functions of water around DOX center of mass in the AA and CG models.

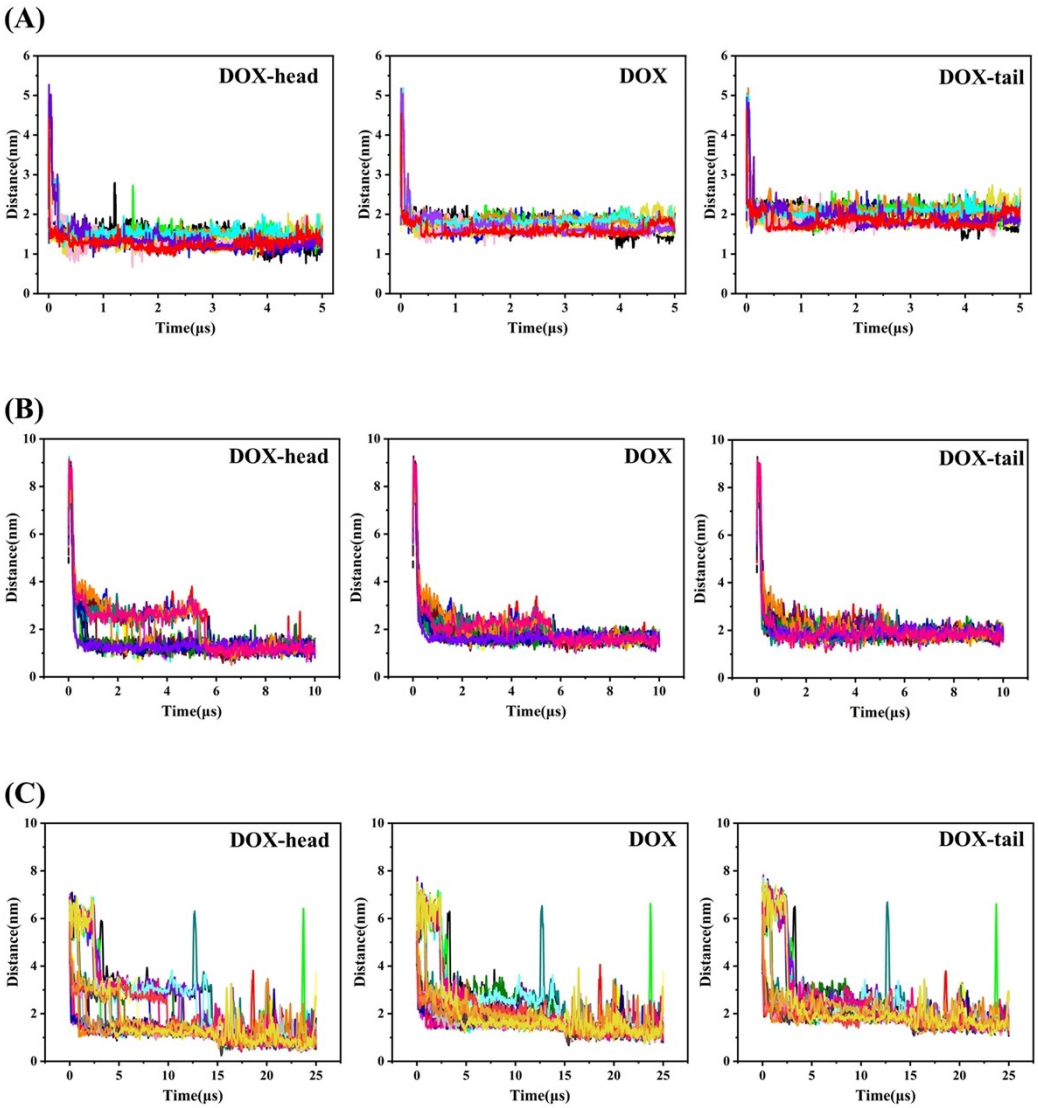

Figure S7. Distance evolutions in z-coordinate of DOX-head, DOX (COM) and DOX-tail with the bilayer center in the different systems. (A) It is Free DOX system and has 10 DOXs. (B)There are 17 DOXs in the PEG2000-DPPE system. (C) 28 DOXs in the PEG1250-DPPE system.

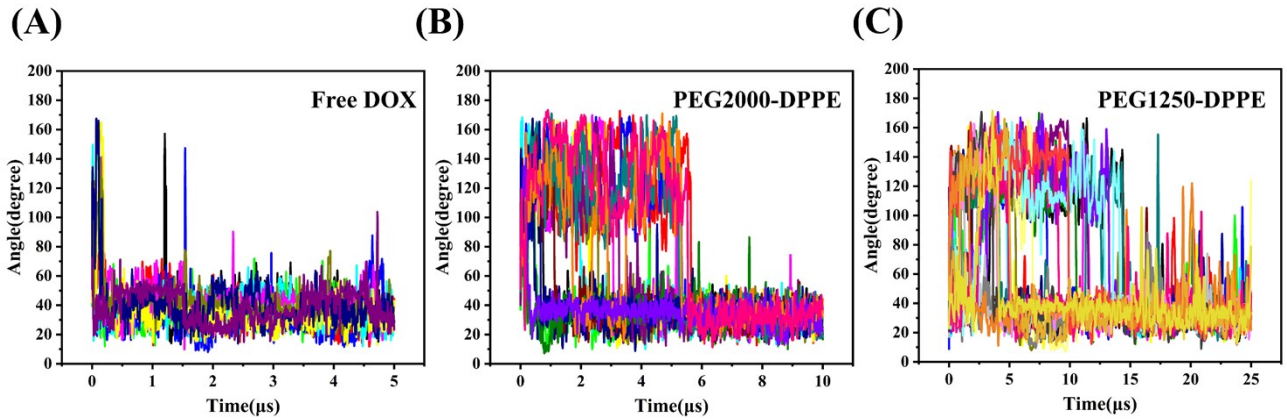

Figure S8. Evolution of the angle of the long axis of DOX relative with the membrane normal over time in different systems. (A) 10 DOXs in the Free DOX system. (B) It is PEG2000-DPPE system

and has 17 DOXs. (C) 28 DOXs in the PEG1250-DPPE system.

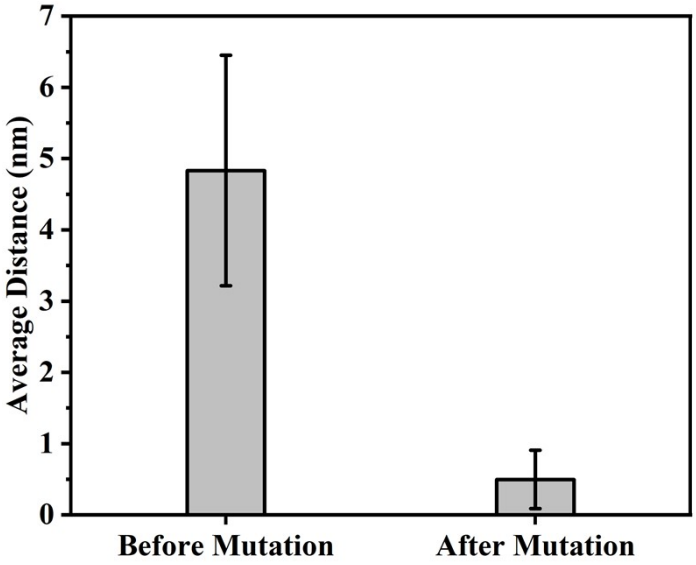

Figure S9. A comparison of the average distance between the core of the micelle and the membrane interior before and after 5.7 μs.

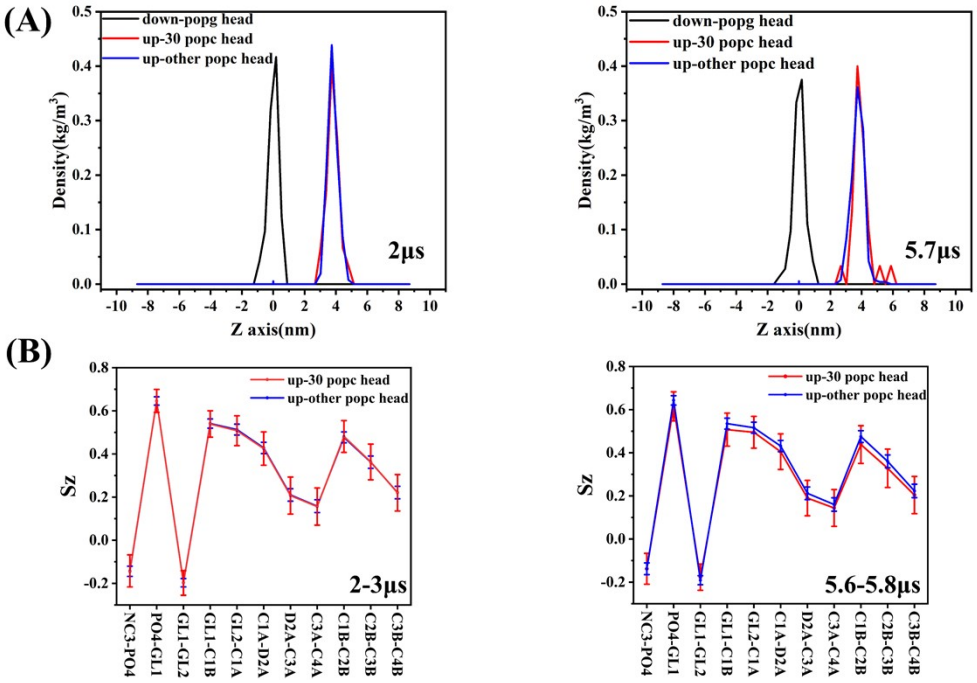

Figure S10. Changes in the distribution and ordering parameters of membrane molecules in the PEG2000-DPPE system. (A) Distribution of lipid molecules in the membrane under deformation and normal conditions. (B) Changes in the ordering parameters of lipid molecules undergoing membrane deformation and under normal conditions. We selected 30 POPC molecules that were brought out near the micelle to calculate the distribution of their heads, and compared them with the heads of other POPC molecules on the same layer. The selected reference position is the head of another layer of POPG molecules, and the thickness of the membrane is 4 nm.

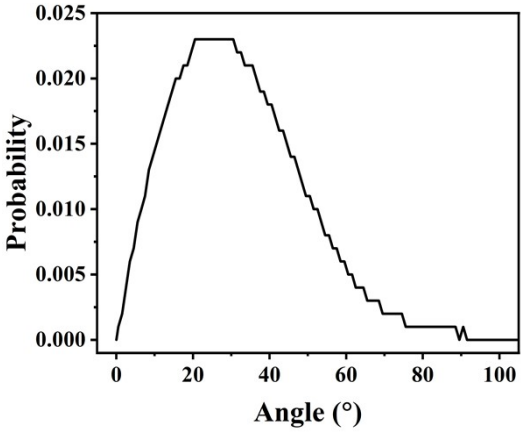

Figure S11. Angle distribution of the long axis of DOX relative with the membrane normal within the last 1 μs. More detailed data of individual DOXs can be seen in Fig. S8.

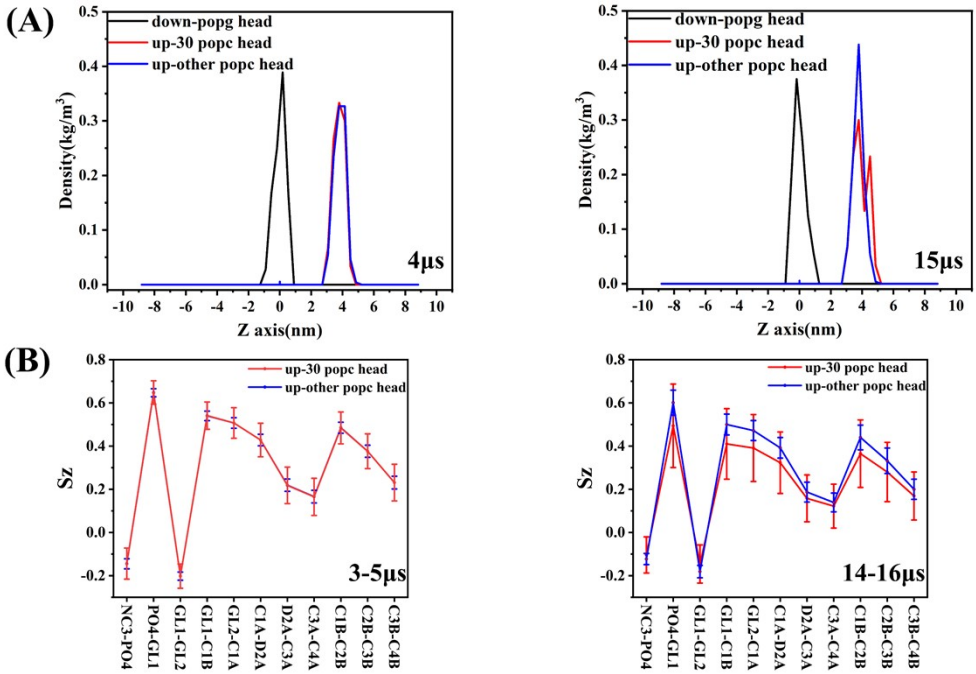

Figure S12. Changes in the distribution and ordering parameters of membrane molecules in the PEG1250-DPPE system. (A) Distribution of lipid molecules in the membrane under deformation and normal conditions. (B) Changes in the ordering parameters of lipid molecules undergoing membrane deformation and under normal conditions. The same method as for the PEG2000-DPPE system was used to calculate the changes in the distribution and ordering parameters of membrane lipid molecules during membrane deformation and under normal conditions.

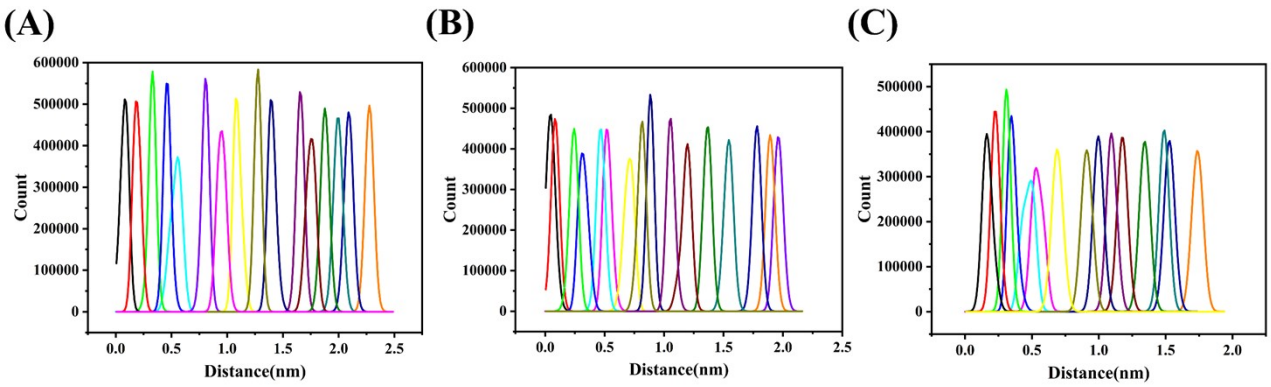

Figure S13. 16 windows were selected for (A) the Free-DOX and (B) the PEG2000-DPPE carrier systems while 15 windows for (C) the PEG1250-DPPE carrier system.

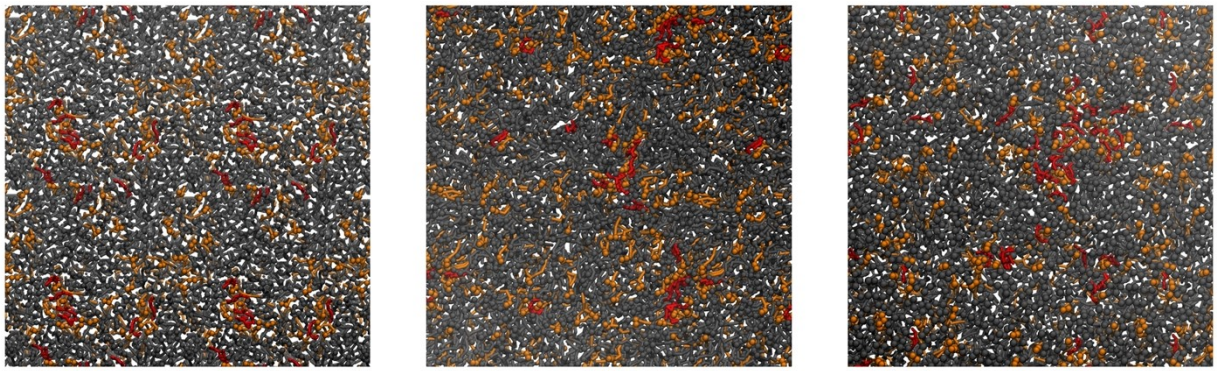

Free DOX **PEG2000-DPPE** **PEG1250-DPPE**

Figure S14. Final distribution of DOXs on the membrane in different systems.

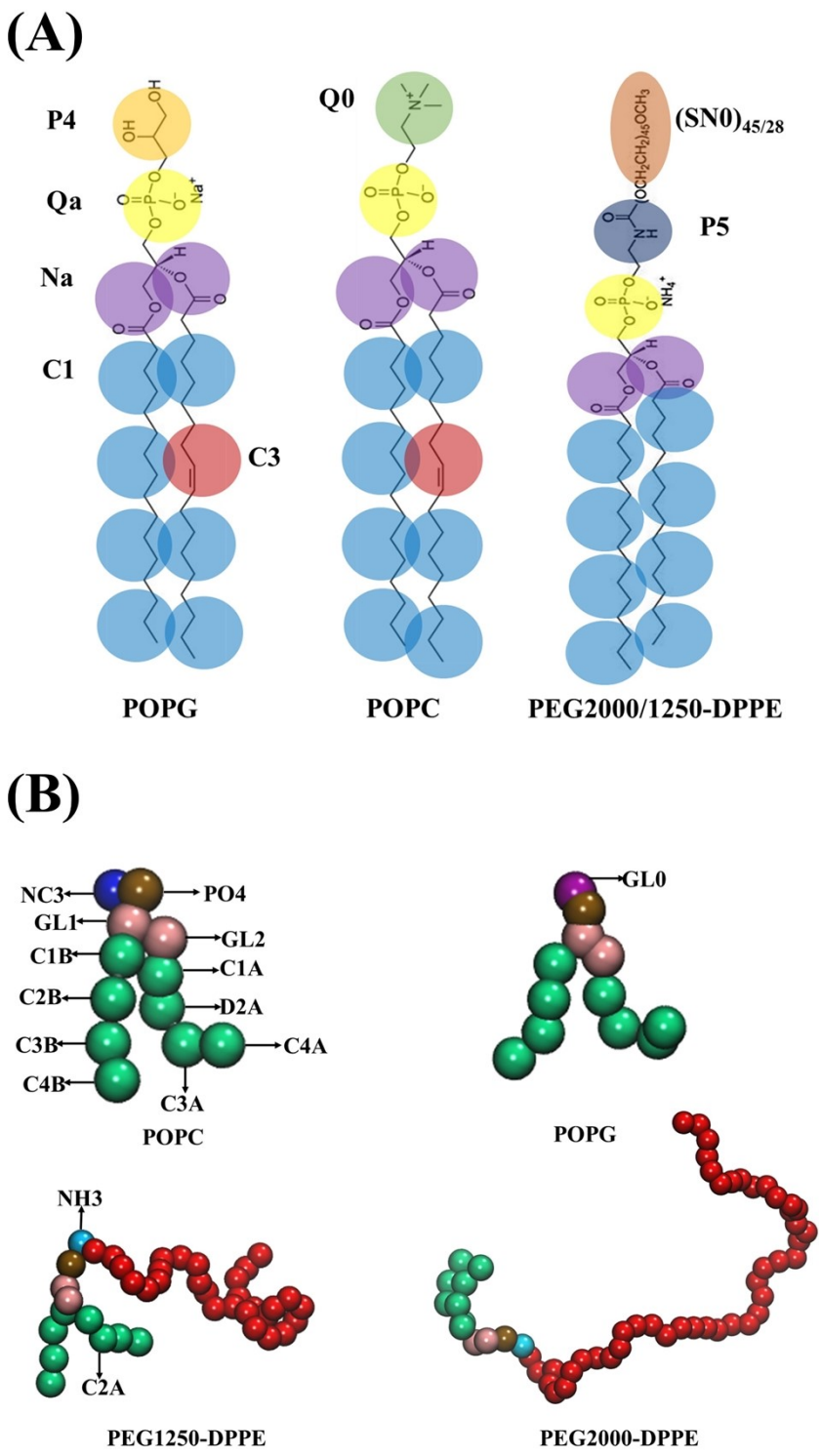

Figure S15. (A) Mapping between the chemical structure and the CG model for POPG, POPC, PEG2000/1250-DPPE. The CG bead types which determine their relative hydrophilicity are indicated. For the structure mapping of PEG2000/1250-DPPE, the CG beads corresponding to the PEG part are replaced by SN0, and the monomer of PEG2000-DPPE includes 45 SN0 beads, and similarly the monomer corresponding to PEG1250-DPPE should contain 28 SN0 beads. (B) The CG model for POPC, POPG, PEG12500-DPPE and PEG2000-DPPE. And we have labeled each bead with its name in the CG model so that it can be better corresponded to its own structure.